

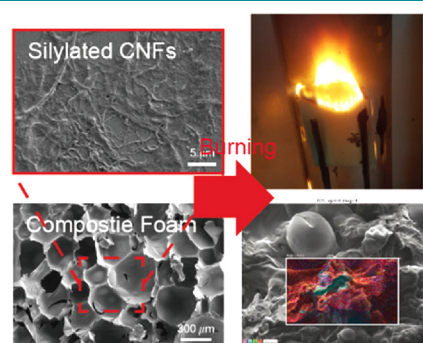
Eco-Friendly Nanocellulose Embedded Polymer Composite Foam for Flame Retardancy Improvement

Hansu Kim^{†,1}
 Juhyuk Park^{†,1}
 Kyung Suh Minn¹
 Jae Ryoun Youn^{*,1}
 Young Seok Song^{*,2}

¹ Research Institute of Advanced Materials (RIAM), Department of Materials Science and Engineering, Seoul National University, 1, Gwanak-ro, Gwanak-gu, Seoul 08826, Korea
² Department of Fiber System Engineering, Dankook University, 152, Jukjeon-ro, Suji-gu, Yongin-si, Gyeonggi 16890, Korea

Received May 11, 2019 / Revised July 1, 2019 / Accepted July 2, 2019

Abstract: Delaying flame propagation in the event of a fire can increase the likelihood of preserving life and alleviating property damage. Here, a strategy for flame retardant polymer composite foam is proposed, which enables the improved performance, good formability, and reduced environmental burden while burning. The strategy is to incorporate silylated nanocellulose into a polyurethane matrix containing a conventional flame retardant, Tris(2-chloroethyl) phosphate (TCEP). This strategy leads to the generation of char layer faster during combustion, resulting in a delayed flame propagation. The limiting oxygen index (LOI) of the samples increased by 28%, and the production rate of toxic gas emission was considerably reduced. The chemical, thermal, mechanical, and morphological analyses were carried out to understand the underlying physics.



Keywords: polyurethane foam, nanocellulose composite, flame retardancy, silylated cellulose.

1. Introduction

As fire safety has emerged as one of the most important issues in recent years, reliable thermal stability of materials acts as a critical factor in designing building materials, electronics, furniture, textiles, etc.¹ Particularly, flame retardancy, which delays or blocks the flame propagation in the event of a fire, is a momentous characteristic directly related to survival of humans.

Flame retardant materials are substances with a sufficiently low flammability causing various physicochemical mechanisms when ignited.^{2,3} Typically, the flame retardant additives are classified into several categories: mineral fillers,⁵ hydrate,⁴ intumescent materials,^{5,6} and organohalogen compounds.⁷ While some retardation mechanisms have been reported such as char formation,⁸ gas phase dilution,⁹ thermal shielding,¹⁰ endothermic degradation,¹¹ and gas phase radical quenching,¹² the theoretical exploration still needs to be conducted.¹³ Rather than used alone, the flame retardant materials are used as an additive to impart flame retardancy to matrices. For instance, various flame retardants are incorporated into polymeric foams which are widely used for industrial applications such as thermal insulation^{14,15} and sound

absorption.¹⁶⁻¹⁹ However, they have caused a great environmental burden due to the toxicity of the materials themselves.²⁰ For example, the organohalogen compounds with aromatic rings are thyroid hormone-destroying agents because their chemical structures are similar to hormones.¹ Therefore, development of materials with high flame retardancy and low toxicity can impose a revolutionary impact to many industries.²¹⁻²³

A nanocomposite design strategy improves material properties by imparting the pre-eminent properties of nanofillers to the matrix.²⁴ Among them, nanocellulose is regarded as an attractive filler for composites because of its characteristics such as eco-friendliness,²⁵ low cost,²⁶ lightweight,²⁷ low thermal conductivity,²⁸ biocompatibility,²⁹ and facile chemical treatment.³⁰

In this sense, nanocellulose embedded composites can demonstrate a variety of advantageous material properties. However, the flammability of nanocellulose hinders practical applications as an insulating material. In our previous study,³¹ it was reported that chemical functionalization *via* silylation allows the nanocellulose to possess flame retardancy.³² When the chemically-treated nanocellulose is burned, carbonized char is generated more actively and delays the flame propagation through the material.³³

In the current study, we developed flame retardant composite foams filled with eco-friendly nanocellulose. When the silylated nanocellulose fibers are embedded in the polyurethane (PU) matrix, the composite foam can provide sufficient flame retardancy with a relatively small amount of conventional flame retardant material. The composite foam also can maintain mechanical and thermal insulation properties, which are normally degenerated by the addition of conventional flame retardant materi-

Acknowledgments: This work was supported by GRR program of Gyeonggi Province (GRR Dankook2016-B03). In addition, this research was supported by Basic Science Research Program through the National Research Foundation of Korea (NRF) funded by the Ministry of Education (2018R1D1A1B07049173) and by the Korea government (MSIT) (No. NRF-2018R1A5A1024127).

*Corresponding Authors: Jae Ryoun Youn (jaeryoun@snu.ac.kr), Young Seok Song (ysong@dankook.ac.kr)

[†]These authors equally contribute to this work.

als. The characteristics of the samples were investigated to understand the enhancement mechanisms.

2. Experimental

2.1. Preparation of flame retardant nanocellulose

Cellulose nanofibers (CNFs), also called nanofibrillated celluloses, were purchased from University of Maine-Process Development Center (United States). Before the usage, CNFs were dispersed in water by stirring for 24 h, ultrasonicated 30 min, and lyophilized in a bid to separate them. The silylation process for imparting flame retardancy to CNFs was performed using MTMS (Methyltrimethoxysilane, 97%, Alfa Aesar, United States). Depending on the mass ratio of CNF and MTMS, three silylated CNF samples were prepared, which were denoted as silylated nanofibrillated celluloses (Si-CNFs) 1 (CNFs:MTMS=1:1), Si-CNFs 2 (1:3), and Si-CNFs 3 (1:5). In this study, the Si-CNFs 3 was selected as an additive embedding in the composite foams because of its good flame retardancy verified in our previous work.³¹

The 5 wt% MTMS/water solution was added dropwise to the 1% CNFs/water solution. The chemical reaction was carried out under aqueous condition while stirring for 130 min. After completion of the reaction, the CNFs/MTMS/water solution was poured into a conical tube and lyophilized to obtain a dried powder of the Si-CNFs samples.

2.2. Fabrication of flame retardant foam

A polyether polyol mixture (MCNS Rigid System Polyol, Mitsui Chemicals & SKC Polyurethanes Inc., Republic of Korea) and polymethylene polyphenyl isocyanate (COSMONATE M-200, Mitsui Chemicals & SKC Polyurethanes Inc., Republic of Korea) were employed as base chemical resins for fabricating polyurethane (PU) foams. 3 wt% of water was added to the polyol mixture as a chemical blowing agent. The two resins were mixed vigorously at 3000 rpm with a 1:1.3 mass ratio of the polyol resin and the isocyanate resin. The mixed resin was poured into an acrylic mold with the dimension of 10 cm×10 cm×5 cm. The amount of poured resin was adjusted to produce a foam of 50 kg/m³ density. The surface of the mold was coated with a demolding agent, AKO-HM207K (Akochem, Republic of Korea). Temperature of the mold was maintained at 60 °C through the foaming reaction. Three different flame retardant foams were fabricated: (i) foam containing only a conventional flame retardant (polyurethane foam/Tris(2-chloroethyl) phosphate, PUF/TCEP), (ii) foam containing only Si-CNFs (PUF/Si-CNFs), and (iii) foam containing both flame retardants (PUF/Si-CNFs/TCEP). 20 wt% of Tris(2-chloroethyl) phosphate (TCEP, Sigma Aldrich, United States), a conventional flame retardant, was added into the polyol mixture. The flame retardant PU composite foams were filled with 5 wt% of the Si-CNFs after the polyol/Si-CNFs was vigorously mixed at 3000 rpm. The PUF/Si-CNFs/TCEP sample was prepared by adding both flame retardants into the polyol mixture. The remaining manufacturing processes were the same as the PU foaming process described above.

2.3. Characterizations

Microstructure morphology of the fabricated samples was observed using a field-emission scanning electron microscope (FE-SEM, MERLIN Compact, ZEISS, Germany). The aqueous solution containing CNFs was dropped onto a silicon wafer, and the water was dried. The foam samples were cut into specimens after freeze-drying with liquid nitrogen to preserve the microcellular structures. The prepared specimens were coated with Pt using a sputter (MSC-101, JEOL, Germany). Energy-dispersive X-ray spectroscopy (EDX) equipped with the FE-SEM was used for the chemical element analysis of the specimens. To investigate the chemical structures of the samples, Fourier transform infrared spectroscopy (Cary 660 FTIR Spectrometer, Agilent, United States) was employed with the Varian Resolutions Pro software. All data were obtained at a resolution of 4 cm⁻¹ from 4000 cm⁻¹ to 650 cm⁻¹. The acquired data were normalized as an arbitrary unit from zero to one to compare the intensities directly. Thermal stability of the samples was examined using a thermogravimetric analyzer (SDT Q600, TA Instruments, Australia). The samples were heated from room temperature to 600°C at a heating rate of 20 °C/min under a nitrogen flow of 100 mL/min. The thermal conductivity of the samples was measured by using a thermal analyzer (C-Therm TCi, C-Therm Technologies Ltd, New Brunswick, Canada). Limiting oxygen index (LOI), a standard of flame retardancy was measured by using a flammability tester based on ASTM D2863/77 (Stanton Redcroft, United Kingdom). Mechanical properties of the foam samples were investigated using a universal testing machine (UTM, WL2100, WITHLAB, Republic of Korea) with a clamp for the compression mode. A cone calorimeter (Cone Calorimeter ISO 5660, Festec International Co. Ltd., Republic of Korea) was used to measure the heat release rate, smoke release, ignition time, oxygen consumption, carbon monoxide and carbon dioxide generation, and mass loss rate. All the prepared samples were conditioned at room temperature and 50% relative humidity for at least 7 days before testing to satisfy equilibrium conditions. A constant irradiation heat flux of 50 kW/m² was irradiated to the testing samples while opening the thermal shutter, and an electric spark was used for ignition. The samples were tested more than twice to validate repeatability.

3. Results and discussion

3.1. Fabrication of PU composite foam

The composite foams with enhanced flame retardancy were made by incorporating flame retardant nanocellulose fillers and a conventional flame retardant, Tris(2-chloroethyl) phosphate (TCEP) into PU foam. We experimentally set the filler contents since TCEP of 20 wt% or more and CNFs of 5 wt% or more affected to dimensional stability of foams. Prior to the fabrication, the flame retardant nanocellulose is prepared through the chemical treatment of silylation. The cellulose nanofibers (CNFs) were prepared by using the same chemical treatment as our previous work employing silylated cellulose nanocrystal (NCC).³¹ In this study, CNFs were chosen since they have several advan-

tages over NCC, such as low thermal conductivity, eco-friendliness, and ease of chemical treatment. The surface of treated CNFs were covered with polysiloxane layers as demonstrated in Figure 1(a). The sample was named as silylated nanofibrilated celluloses (Si-CNFs). The chemical treatment can enhance the amount of generated chars during burning.³¹ The polyurethane foams (PUFs) were fabricated using foam reaction molding method where polyol and isocyanate resins are mixed vigorously and poured into a mold for curing. We fabricated four different samples: neat PUF, PUF/Si-CNFs, PUF/TCEP, and PUF/Si-CNFs/TCEP as shown in Figure 1(b). Details about the method are described in the experimental section.

The microcellular structure of the composite foam was observed with an FE-SEM (field emission scanning electron microscope) (Figure 1c). The average cell diameter of the neat PUF was $416.9 \pm 55.6 \mu\text{m}$ (Figure 1(c)-(i)). The critical energy required for nucleation can be lowered significantly on the surface of the nanosize particles.¹⁹ Therefore, the presence of the Si-CNFs in the resin mixture provoked uniform microcellular distribution in the PUF during foaming reaction, resulting in a mean cell diameter of $266.5 \pm 68.7 \mu\text{m}$ (Figure 1(c)-(ii)). On the contrary, TCEP increased the cell size (*i.e.*, the average cell diameter of $488.3 \pm 82.3 \mu\text{m}$, Figure 1(c)-(iii)), since it reacted with the cyanate groups of the resin and changed the balance between the foaming and the

gelling reactions. This phenomenon weakens the mechanical stiffness of the foam samples, which is why TCEP is not generally used for flame retardancy as a single additive. Moreover, the PU resin and TCEP mixture has low blowing rate during foaming reaction, resulting in poor formability. On the other hand, the combination of Si-CNFs and TCEP increased the cell nucleation rate as shown in Figure 1(c)-(iv) (the average cell diameter, $327.6 \pm 76.4 \mu\text{m}$). Since the Si-CNFs increased the viscosity of the resin mixture during foaming reaction, the growth of microcells were more stable. In addition, increase in the nucleation rate due to the nanocellulose fillers led to good formability.

Chemical structure of the samples was investigated using the FTIR (Fourier-transform infrared spectroscopy) spectra (Figure 1(d)). In the neat PUF FTIR spectra, the broad peak near 3400 cm^{-1} indicates hydroxyl moieties on the molecular chain of the polyol-based resin. The peak at 1708 cm^{-1} corresponds to the C=O bond in the ester moiety (RCOOR') of the polyol-based resin and urethane linkage moiety (R-NHCOO-R'). The urea linkage peak is shown at 1412 cm^{-1} , indicating the gelling reaction between hydroxyl groups and cyanate groups.³⁴

The peaks found at 2970 cm^{-1} , 2872 cm^{-1} , 1595 cm^{-1} , and 1073 cm^{-1} are due to CH_3 vibration, CH_2 vibration, aromatic ring, and C-O bond, respectively.³⁵ For the samples containing Si-CNFs, a slightly overlapped broad absorption peak in the $1000\text{--}1100$

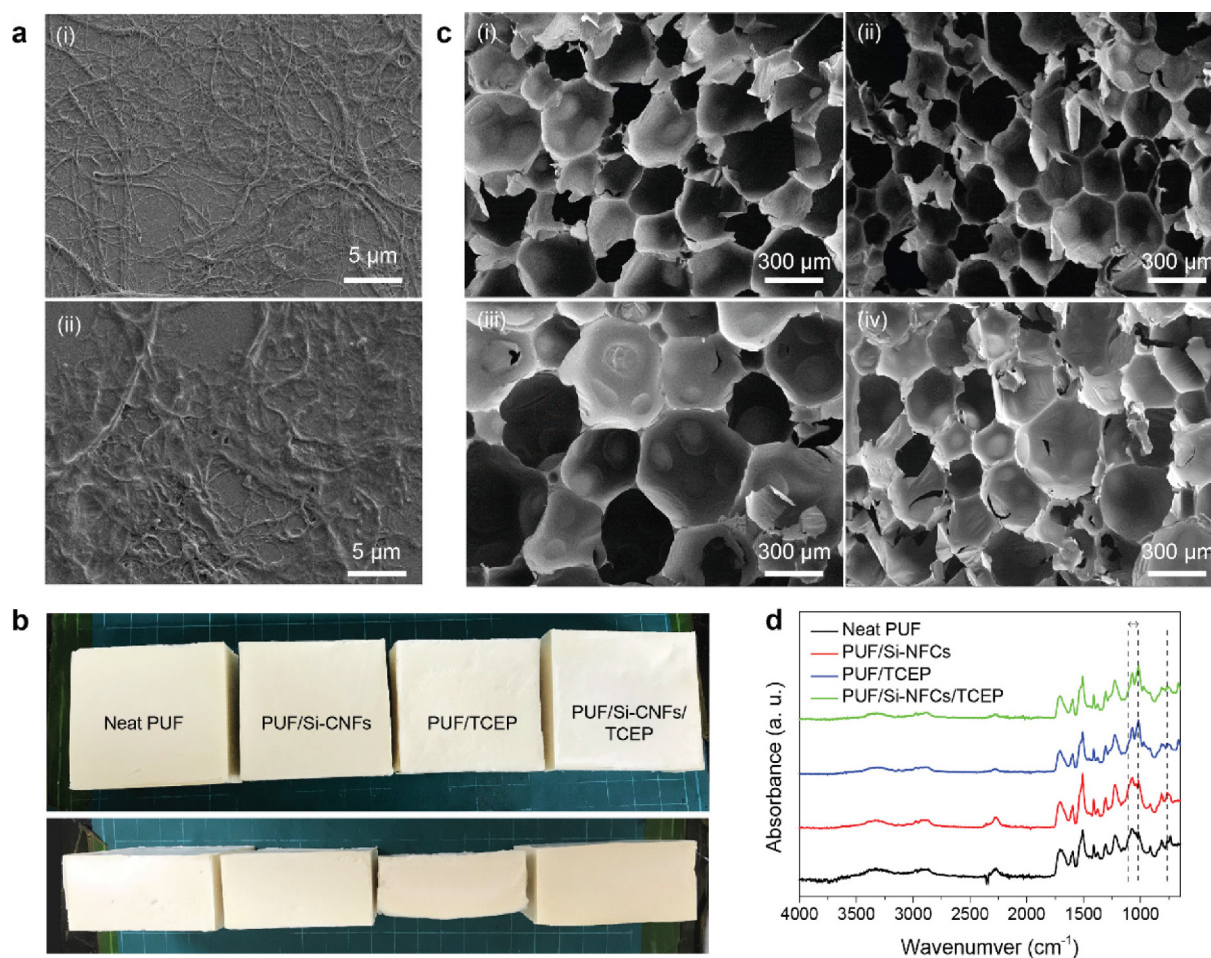


Figure 1. Fabricated polyurethane/silylated nanocellulose composite foams. (a) Morphology of (i) the neat CNFs and (ii) the silylated CNFs (Si-CNFs). (b) Optical photographs of the fabricated foams. (c) Microcellular structures of the fabricated foams for (i) the neat PUF, (ii) the PUF/Si-CNFs, (iii) the PUF/TCEP, and (iv) the PUF/Si-CNFs/TCEP samples. (d) FTIR spectra of the samples.

cm^{-1} region is discovered due to the Si-O-Si bonds by silylation. The FTIR peak of the Si-C bond is observed at 762 cm^{-1} . On the other hand, the phosphorus-related peaks at 1308 cm^{-1} and 1015 cm^{-1} indicating P=O and P-O-C bonds were found in the samples incorporating TCEP, the PUF/TCEP and PUF/Si-CNFs/TCEP. From the FTIR analysis, it was verified that the overall chemical structure of the embedded chemicals and fillers are preserved without undesired modifications.

3.2. Thermal and mechanical properties

Thermal stability of the sample was examined through TGA (thermogravimetric analysis) under N_2 environment, so as not to ignite but to carbonize the sample by thermal decomposition (Figure 2(a), (b)). The thermal stability of the neat PUF was improved by adding the Si-CNFs. The final residue after heating the samples up to $700\text{ }^\circ\text{C}$ (3.7 wt%) was increased by 2.8 times compared with the PUF/Si-CNFs sample (10.5 wt%). Since the thermal conductivity of Si-CNF is lower than that of polyurethane matrix, embedding the Si-CNFs can enhance the thermal stability of the PUF.³⁶ Furthermore, our previous study reported that the silylation treatment of CNFs enhanced the thermal stability.³¹ Incorporation of TCEP into the PU matrix similarly increased the residual char at the final temperature of $700\text{ }^\circ\text{C}$ (12.2 wt%) and lowered the thermal stability of the PUF compared with the neat PUF in the temperature range from 200 to $400\text{ }^\circ\text{C}$. The TCEP molecules were thermally decomposed at the relatively low temperature range due to the generation of P-O-C and P-C to form phosphinic acid before the collapse of PU chains. This

might have adverse effects on thermal stability of the PUF, but the residue of the PUF/TCEP sample increased by about 1.5 times compared with that of the neat PUF when heated up to $700\text{ }^\circ\text{C}$. Its major mechanism is explained by the formation of carbonized layer after rapid thermal decomposition, which blocks heat transfer from the outside and facilitates char formation. The residual char of the PUF/Si-CNFs/TCEP sample was improved synergistically, which is larger than that of the neat PUF sample by about 5 times when heated up to $700\text{ }^\circ\text{C}$. This is a meaningful result for industrial applications since the thermal stability of the material is important in the event of a fire. Figure 2(b) shows the differential curves of the TGA thermograms for the four samples.

Mechanical stiffness of the samples was measured by using a UTM (universal test machine) in a compression mode, and the results were compared as shown in Figure 2(c). The compressive stress-strain (S-S) curve of the neat PUF was compared with the curve of the PUF/Si-CNFs. It is well known that nanoscale fillers reinforce the matrix material due to their exceptional aspect ratio and large surface area. Although the silylation treatment on CNFs might reduce the mechanical properties compared with the use of pristine CNFs, the elastic modulus of the PUF/Si-CNFs (25.0 MPa) is greater than that of the neat PUF (17.1 MPa) by 1.5 times. On the contrary, the addition of TCEP into PUF lowered the elastic modulus of the foam by 1.7 times (10.0 MPa). It is presumed that the TCEP intercalated in the resin hinders the gelling reaction between -OH and -NCO and deteriorates the stiffness of the PUF. Accordingly, the molecular weight of the resin was lowered. Adopting both Si-CNFs and TCEP

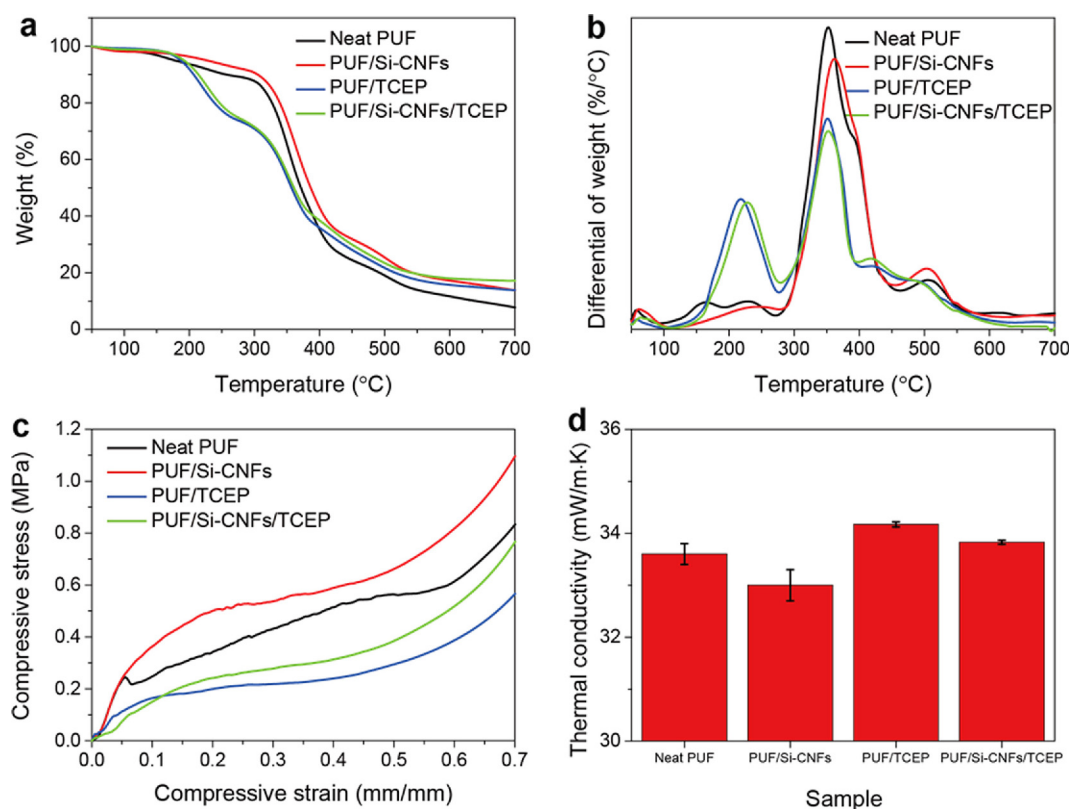


Figure 2. Thermal and mechanical properties of the fabricated composite foams. (a) TGA thermogram, (b) DTGA, (c) compressive stress-strain curves, and (d) thermal conductivities of the samples.

compensated this shortcoming and improved the mechanical property of the composite foams by achieving the elastic modulus of 12.1 MPa for the PUF/Si-CNFs/TCEP sample.

Thermal conductivity is one of the most important properties of building materials such as PUF. Many studies have been conducted to improve the thermal insulation performance of porous materials by tuning microcellular structures while other macroscopic properties remain unchanged.^{37,38} The thermal conductivity of the neat PUF was 33.6 mW/m·K, which is a typical value for conventional PU foams (Figure 2(d)). Embedding Si-CNFs in the PUF decreased the thermal conductivity slightly. This decrease in thermal conductivity can be explained by two mechanisms; structural change to smaller and more uniform cell size distribution (Figure 1(c)-(ii)) and altered material composition. The foams with small microcellular sizes have been reported to show good thermal insulation,³⁸ and furthermore, thermal conductivity of the cellulose material itself is slightly lower than that of PU matrix.³⁹ Meanwhile, TCEP induces relatively large and non-uniform microcells (Figure 1(c)-(iii)), which resulted in poor thermal insulation. It was found that the insulation property of the PUF/Si-CNFs/TCEP sample is similar to that of the neat PUF (Figure 1(c)-(iv) and Figure 2(d)).

3.3. Flame retardancy test

Flame retardancy was investigated by conducting a low oxygen index (LOI) test (Figure 3(a)). The right picture in Figure 3(a) shows how to measure the LOI value. The LOI value of the neat PUF was about 21%, which is the typical value of porous

polymers. Since atmospheric oxygen concentration is the same as the LOI value of the neat PUF (about 21%), fire on the PUF is not extinguished easily.

CNF is a combustible material which is not used as a flame retardant because it contains hydrocarbon chains. However, the silylation treatment of CNF converted this combustible material into a flame retardant material by increasing the production rate of char during combustion due to the generated Si-O and Si-C groups on CNFs (e.g., the LOI value of around 35%).³¹ Incorporating Si-CNFs into the matrix increased the LOI up to 22%. Since the value is larger than the atmospheric oxygen concentration. It is expected that larger amount of Si-CNFs in polymer matrix would offer better flame retardancy. However, this expectation was not verified experimentally because the resin viscosity increased dramatically when more than 5 wt% Si-CNFs were added to the polyol-based resin. When the LOI test was conducted for the neat PUF sample, color of the smoke was deep-black, which indicates incomplete combustion. Under the presence of Si-CNFs in the PUF, the reaction balance between the PU combustion and supply of oxygen is changed by generating Si-C and Si-O bonds, and then the smoke color became white upon burning.

On the other hand, the TCEP chemical is one of the most frequently used flame retardant due to its outstanding performance. Phosphate atoms of TCEP can hinder the transfer of reactive radicals to polymeric chains and then prevent the propagation of flames into the material. As expected, the PUF/TCEP showed a superior flame retardancy, the LOI value of 25%. Despite this good performance, the use of TCEP is strongly sublated due to

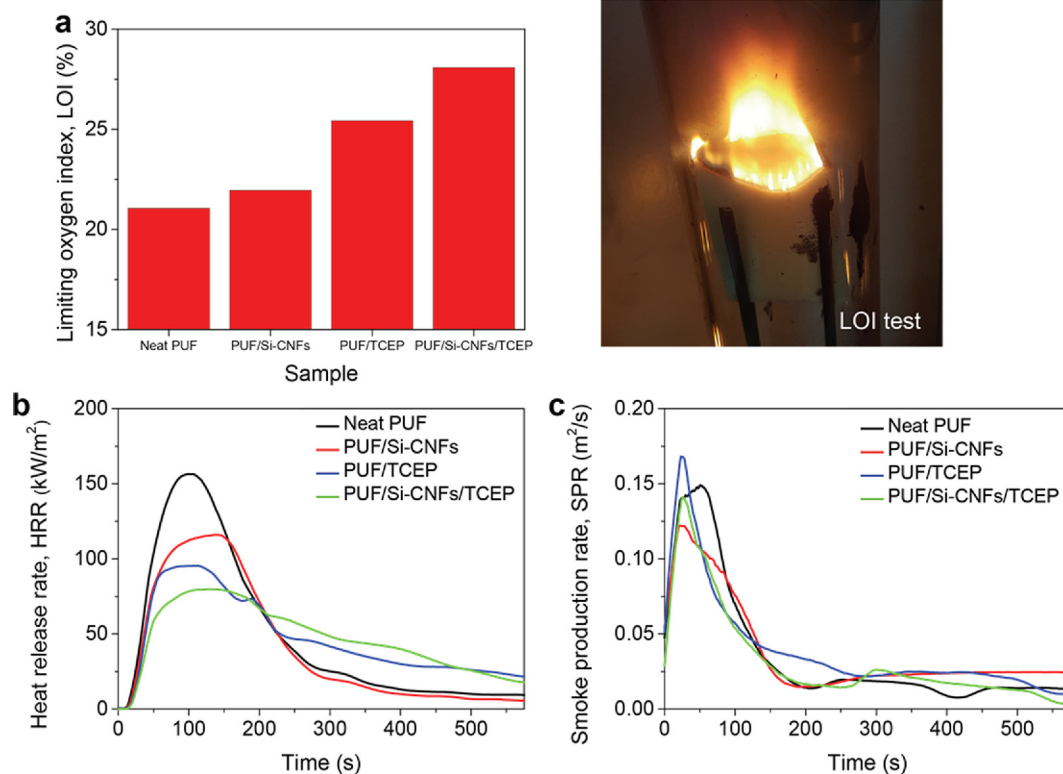


Figure 3. Flame retardancy of the synergetic composite foams. (a) Limiting oxygen index (LOI) results of the fabricated foams (left) and the photograph of the LOI test (right), (b) time-dependent heat release rate (HRR), and (c) smoke production rate (SPR) of the samples while burning in the cone calorimetry.

environmental problems and health hazards, which are caused by the extremely toxic gases generated during combustion. In this sense, we fabricated hybrid composite foams by combining Si-CNFs with TCEP. Interestingly, the LOI value of the PUF/Si-CNFs/TCEP composite foam was measured as over 28%, which is higher than the weighted mean of LOI values of the two additives. This synergistic effect was realized by the rapid char formation and the protection of polymeric chains through blocking the radical transfer at the same time in the PU matrix upon burning.

The heat release rate (HRR) and smoke production rate (SPR) of the samples were measured by the cone calorimeter to investigate the physics of combustion (Figure 3(b), (c)). The HRR value implies the rate of heat generation upon fire indicates the flammability, which is proportional to the oxygen consumption. The total heat released through burning is the same for the samples because of the same calorific value for each sample upon fire. The peaks of HRR values of the neat PUF, PUF/Si-CNFs, PUF/TCEP, PUF/Si-CNFs/TCEP samples were varied from 156 kW/m², 122 kW/m², 95 kW/m², to 78 kW/m², respectively. A low HRR value means that the propagation speed of heat along the external flame is slow. Compared with the neat PUF, the PUF/Si-CNFs/TCEP had a half HRR value due to the synergistic effect. On the other hand, the SPR value is a measure of the rate of generation of toxic gases during combustion that can pose a threat to life and environment.⁴⁰ The presence of TCEP in the PU foam accelerated the smoke generation, which is the emission of radical from the burnt TCEP (Figure 3(c)). The Si-CNFs lowered the peak of smoke production rate (SPR) value of the PUF/Si-CNFs/TCEP sample to the PUF/TCEP level. In this way, Si-CNF can help flame

retardancy of TCEP.

The structural features of the ash remaining after burning were observed to account for the improved flame retardancy from a different perspective. The macroscopic images of the burned samples were demonstrated in Figure 4(a). Compared with the samples without Si-CNFs, other samples showed a relatively high structural stability after the cone calorimeter test. The formation of a siliceous char by Si-CNFs maintained the morphological dimension of the samples unlike the neat PUF. Also, the fired PUF/TCEP and PUF/Si-CNFs/TCEP samples were formed with the intumescent char layers.⁴¹ This characteristic is useful for designing a fire safe building because the collapse time of buildings can be delayed by blocking flame. This improved structural robustness can be understood by assessing the microstructures of the samples (Figure 4(b)-(e)). From the SEM images of the samples with Si-CNFs, the sample surfaces were entirely covered with a rigid-looking layer consisting of char, Si-C, and SiO₂. The EDX images revealed that the flame retardancy of the foam composite was affected considerably by the existence of silicon atoms (Si-C and SiO₂) although Si-CNFs were agglomerated in the sample surfaces. Meanwhile, the neat PUF and PUF/TCEP samples were wrapped by a porous layer without Si. The phosphorus atoms were evenly located on the entire surface of the samples with TCEP. The uniform distribution of phosphorus element on the surface ensured better flame retardancy by producing intumescent char layers formed by the bonds of P=O and P-O-C. Consequently, the synergistic effect of flame retardation was confirmed by the structural stability due to the formation of rigid char layers and the lagging of radical propagation rate inside the polymer backbone.

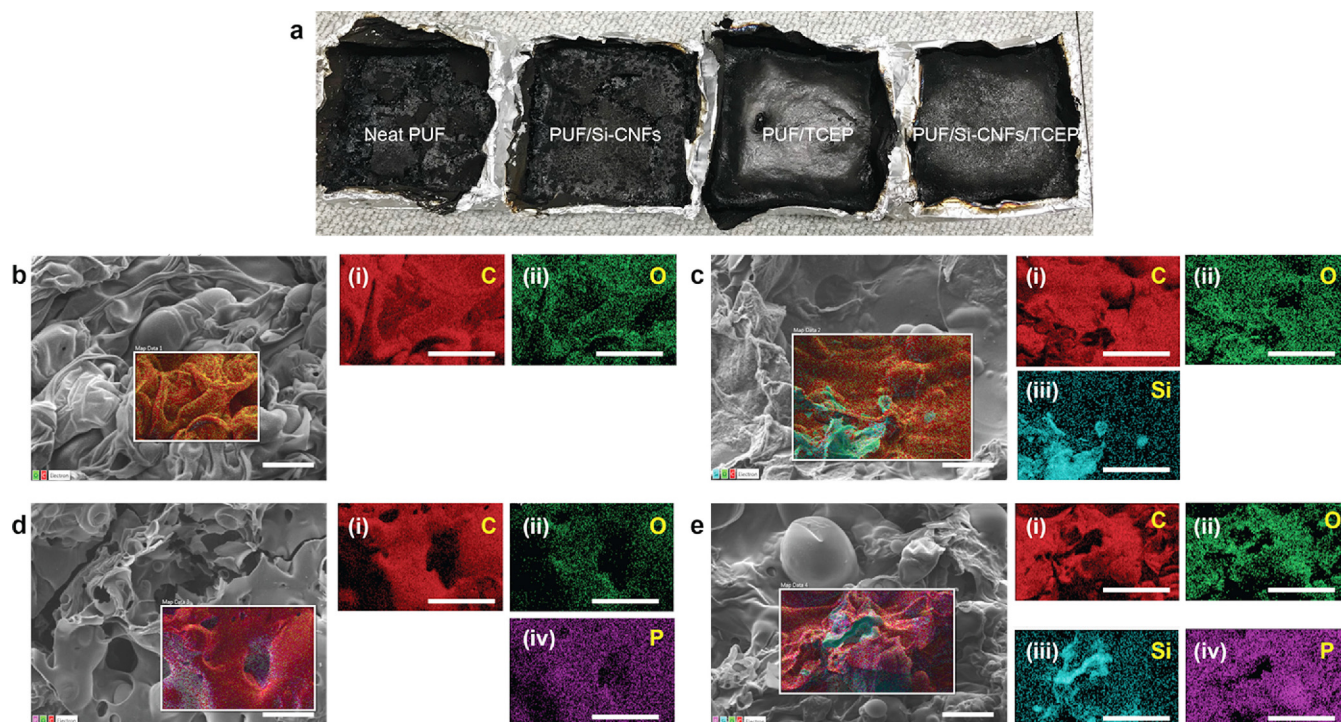


Figure 4. Macro/microscopic analyses of the burned samples. (a) Macroscopic pictures after burning. Microscopic SEM images and EDX data of (b) the neat PUF, (c) PUF/Si-CNFs, (d) PUF/TCEP, and (e) PUF/Si-CNFs/TCEP samples after burning. Each right sub-figure displays (i) C K line, (ii) O K line, (iii) Si K line, and (iv) P K line. The error bar indicates 100 μm .

3. Conclusions

In this study, we fabricated a flame retardant polyurethane composite foam incorporated with Si-CNFs. Addition of Si-CNFs into the PUF led to the reduction in cell size and the homogenous microcellular structure by accelerating the rate of cell nucleation in the PU matrix. This structural advantage prevented the deterioration of the mechanical strength and thermal insulation. Combining Si-CNFs with TCEP opens a way to obtain high flame retardancy, *i.e.*, the high LOI value of 29%, while reducing existing flame retardant agent. In addition, Si-CNFs increased the moldability of the PU resin containing TCEP. In the cone calorimetry test, low HRR and SPR values were obtained for the PUF/Si-CNFs/TCEP sample, implying both high flame retardancy and relatively lowered environmental burden. The membrane covering the burned sample surface was structurally investigated. The strategy proposed in this study will provide a way for reducing environmental burden of insulating materials and improving flame retardant performance.

References

- (1) S. Shaw, *Rev. Environ. Health.*, **25**, 261 (2010).
- (2) K. Wu, Y. Hu, L. Song, H. Lu, and Z. Wang, *Ind. Eng. Chem. Res.*, **48**, 3150 (2009).
- (3) X. Wang, L. Song, H. Yang, H. Lu, and Y. Hu, *Ind. Eng. Chem. Res.*, **50**, 5376 (2011).
- (4) S. Li, C. Li, C. Li, M. Yan, Y. Wu, J. Cao, and S. He, *Polym. Degrad. Stab.*, **98**, 1940 (2013).
- (5) S. Vecchiato, L. Skopek, S. Jankova, A. Pellis, W. Ipsmiller, A. Aldrian, B. Mueller, E. H. Acero, and G. M. Guebitz, *ACS Sustain. Chem. Eng.*, **6**, 2386 (2017).
- (6) M. Jimenez, S. Duquesne, and S. Bourbigot, *Ind. Eng. Chem. Res.*, **45**, 4500 (2006).
- (7) I. Van der Veen and J. de Boer, *Chemosphere*, **88**, 1119 (2012).
- (8) J. H. Cho, V. Vasagar, K. Shanmuganathan, A. R. Jones, S. Nazarenko, and C. Ellison, *Chem. Mater.*, **27**, 6784 (2015).
- (9) T. R. Hull, A. Witkowski, and L. Hollingbery, *Polym. Degrad. Stab.*, **96**, 1462 (2011).
- (10) L. Kong, H. Guan, and X. Wang, *ACS Sustain. Chem. Eng.*, **6**, 3349 (2018).
- (11) L. Hollingbery and T. Hull, *Thermochim. Acta*, **509**, 1 (2010).
- (12) L. Qian, Y. Qiu, J. Wang, and W. Xi, *Polymer*, **68**, 262 (2015).
- (13) Y.-Q. Shi, T. Fu, Y.-J. Xu, D.-F. Li, X.-L. Wang, and Y.-Z. Wang, *Chem. Eng. J.*, **354**, 208 (2018).
- (14) J. Zhao, Q. Zhao, C. Wang, B. Guo, C. B. Park, and G. Wang, *Mater. Des.*, **131**, 1 (2017).
- (15) H. M. Kim, Z. M. Huang, J. S. Kim, J. R. Youn, and Y. S. Song, *Eur. Polym. J.*, **106**, 188 (2018).
- (16) J. Park, H. M. Kim, J. R. Youn, and Y. S. Song, *Adv. Mater. Technol.*, 1800410 (2018).
- (17) J. H. Park, K. S. Minn, H. R. Lee, S. H. Yang, C. B. Yu, S. Y. Pak, C. S. Oh, Y. S. Song, Y. J. Kang, and J. R. Youn, *J. Sound Vib.*, **406**, 224 (2017).
- (18) J. Park, S. H. Yang, K. S. Minn, C. B. Yu, S. Y. Pak, Y. S. Song, and J. R. Youn, *Mater. Des.*, **142**, 212 (2018).
- (19) J. H. Park, S. H. Yang, H. R. Lee, C. B. Yu, S. Y. Pak, C. S. Oh, Y. J. Kang, and J. R. Youn, *J. Sound Vib.*, **397**, 17 (2017).
- (20) P. O. Darnerud, *Environ. Int.*, **29**, 841 (2003).
- (21) C. Luo, J. Zuo, F. Wang, Y. Yuan, F. Lin, and J. Zhao, *Macromol. Res.*, **26**, 346 (2018).
- (22) H. Ding, K. Huang, S. Li, L. Xu, J. Xia, and M. Li, *Polym. Test.*, **62**, 325 (2017).
- (23) M. Ba, B. Liang, and C. Wang, *Fibers Polym.*, **18**, 907 (2017).
- (24) J. Park, J. R. Youn, and Y. S. Song, *ACS Appl. Mater. Interfaces*, **9**, 44724 (2017).
- (25) T. Kovacs, V. Naish, B. O'Connor, C. Blaise, F. Gagné, L. Hall, V. Trudeau, and P. Martel, *Nanotoxicology*, **4**, 255 (2010).
- (26) D. M. Fox, J. Lee, M. Zammarano, D. Katsoulis, D. V. Eldred, L. M. Haverhals, P. C. Trulove, C. Hugh, and J. W. Gilman, *Carbohydr. Polym.*, **88**, 847 (2012).
- (27) N. T. Cervin, L. a. Andersson, J. B. S. Ng, P. Olin, L. Bergström, and L. Wågberg, *Biomacromolecules*, **14**, 503 (2013).
- (28) B. Wicklein, A. Kocjan, G. Salazar-Alvarez, F. Carosio, G. Camino, M. Antonietti, and L. Bergström, *Nat. Nanotechnol.*, **10**, 277 (2015).
- (29) A. Liu and L. A. Berglund, *Eur. Polym. J.*, **49**, 940 (2013).
- (30) Z. Zhang, P. Tingaut, D. Rentsch, T. Zimmermann, and G. Sèbe, *ChemSusChem*, **8**, 2681 (2015).
- (31) H. Kim, J. R. Youn, and Y. S. Song, *Nanotechnology*, **29**, 455702 (2018).
- (32) O. Köklükaya, F. Carosio, and L. Wågberg, *ACS Appl. Mater. Interfaces*, **9**, 29082 (2017).
- (33) Y. Cheng, G. He, A. Barras, Y. Coffinier, S. Lu, W. Xu, S. Szunerits, and R. Boukherroub, *Chem. Eng. J.*, **331**, 372 (2018).
- (34) L. Jiao, H. Xiao, Q. Wang, and J. Sun, *Polym. Degrad. Stab.*, **98**, 2687 (2013).
- (35) X. Chen, L. Huo, C. Jiao, and S. Li, *J. Anal. Appl. Pyrolysis*, **100**, 186 (2013).
- (36) J. Lubczak and E. Chmiel, *Macromol. Res.*, **27**, 543 (2019).
- (37) M. S. Koo, K. Chung, and J. R. Youn, *Polym. Eng. Sci.*, **41**, 1177 (2001).
- (38) C. Kim and J. R. Youn, *Polym. Plast. Technol. Eng.*, **39**, 163 (2000).
- (39) M. Floros, L. Hojabri, E. Abraham, J. Jose, S. Thomas, L. Pothan, A. L. Leao, and S. Narine, *Polym. Degrad. Stab.*, **97**, 1970 (2012).
- (40) S. T. McKenna and T. R. Hull, *Fire Sci. Rev.*, **5**, 3 (2016).
- (41) X. Liu, K. A. Salmeia, D. Rentsch, J. Hao, and S. Gaan, *J. Anal. Appl. Pyrolysis*, **124**, 219 (2017).

Publisher's Note Springer Nature remains neutral with regard to jurisdictional claims in published maps and institutional affiliations.